PHYSICAL REVIEW E **91**, 050104(R) (2015)

Convex hull of a Brownian motion in confinement

Marie Chupeau,[1] Olivier Bénichou,[1] and Satya N. Majumdar[2]
[1]*Laboratoire de Physique Théorique de la Matière Condensée (UMR CNRS 7600), Université Pierre et Marie Curie, 4 Place Jussieu, 75255 Paris Cedex, France*
[2]*CNRS, LPTMS, Université Paris-Sud, 91405 Orsay Cedex, France*
(Received 8 December 2014; published 22 May 2015)

We study the effect of confinement on the mean perimeter of the convex hull of a planar Brownian motion, defined as the minimum convex polygon enclosing the trajectory. We use a minimal model where an infinite reflecting wall confines the walk to one side. We show that the mean perimeter displays a surprising minimum with respect to the starting distance to the wall and exhibits a nonanalyticity for small distances. In addition, the mean span of the trajectory in a fixed direction $\theta \in]0,\pi/2[$, which can be shown to yield the mean perimeter by integration over θ, presents these same two characteristics. This is in striking contrast to the one-dimensional case, where the mean span is an increasing analytical function. The nonmonotonicity in the two-dimensional case originates from the competition between two antagonistic effects due to the presence of the wall: reduction of the space accessible to the Brownian motion and effective repulsion.

DOI: 10.1103/PhysRevE.91.050104 PACS number(s): 05.40.Jc, 05.40.Fb

How does one characterize the territory covered by a Brownian motion in two dimensions? This question naturally arises in ecology where the trajectory of an animal during the foraging period is well approximated by a Brownian motion [1,2] and one needs to estimate the home range of the animal, i.e., the two-dimensional (2D) space over which the animal moves around over a fixed period of time [3]. The most versatile and popular method to characterize the home range consists of drawing the convex hull, i.e., the minimum convex polygon enclosing the trajectory of the animal [4,5]. The size of the home range is then naturally estimated by the mean perimeter or the mean area of the convex hull.

For a single planar Brownian motion of duration t and diffusion constant D, the mean perimeter $\langle L(t)\rangle = \sqrt{16\pi Dt}$ and the mean area $\langle A(t)\rangle = \pi Dt$ were computed exactly in the mathematics literature quite a while back [6–8]. Very recently, there has been a growing number of articles in both the physics [9–15] and the mathematics literature [16–19] generalizing these results in various directions. In particular, adapting Cauchy's formula [20] for closed 2D convex curves to the case of random curves, a general method was recently proposed [9,10] to compute the mean perimeter and the mean area of the convex hull of any arbitrary stochastic process in two dimensions. In cases where the process is isotropic in two dimensions, the mean perimeter and the mean area of its convex hull can be mapped onto computing the extremal statistics of the corresponding one-dimensional component process [9,10]. This procedure was then successfully used to compute exactly the mean perimeter and the mean area of a number of isotropic 2D stochastic processes such as N independent Brownian motions [9,10], random acceleration process [11], and branching Brownian motion with absorption with applications to epidemic spread [12] and for anomalous diffusion processes [14].

All these results pertain to isotropic stochastic processes in the unconfined 2D geometry. However, in many practical situations, the stochastic process takes place in a confined geometry. For example, the home range of animals living in a habitat can get limited by the presence and development of urban areas nearby that may impede the free movement of animals. How does the confinement of the allowed space affect the size of the home range? Beyond this ecological motivation, determining the mean perimeter of the convex hull in confinement is a key question in the context of Brownian motion theory.

In this Rapid Communication, we address this important issue in a simple minimal model that allows an exact solution. We consider a single planar Brownian motion in the presence of a reflecting infinite wall that confines the Brownian motion in the positive half space [see Fig. 1(a)]. This can simply model the habitat of an animal bordering, on one side, a highway or a river that the animal cannot cross. In the presence of this reflecting wall, various properties of the Brownian motion can be calculated analytically (e.g., [21,22]). For instance, it is easy to solve the Fokker-Planck equation to derive the full probability distribution of the position of the particle and all its moments, including, e.g., the mean square displacement. However, these standard methods are neither sufficient nor relevant for the computation of the mean perimeter of the convex hull of the particle up to time t. The observable we are interested in, namely, the perimeter of the convex hull, is a nonlocal history dependent quantity, and calculating even its first moment is nontrivial. One of the main objectives of this Rapid Communication is to demonstrate how to compute this quantity in the presence of a reflecting wall.

We show that the presence of the wall breaks the isotropy of the 2D space in a way that, even in this simple setting, induces a nontrivial effect on the convex hull of the Brownian motion. We compute analytically the mean perimeter $\langle L_{2\mathrm{D}}^{(d)}(t)\rangle$ of the convex hull of the Brownian motion of duration t, starting at an initial distance d from the wall. We show that it exhibits a scaling form, at all times t,

$$\left\langle L_{2\mathrm{D}}^{(d)}(t)\right\rangle = \sqrt{D\,t}\,\tilde{L}_{2\mathrm{D}}\left(\frac{d}{\sqrt{D\,t}}\right), \tag{1}$$

where $\tilde{L}_{2\mathrm{D}}(x)$ is a nontrivial scaling function that we compute explicitly and is plotted in Fig. 1(b). We find a *surprising*, and rather striking, nonmonotonic behavior of the scaling function $\tilde{L}_{2\mathrm{D}}(x)$, revealing a minimum at a certain characteristic scaled distance [see Fig. 1(b)]. Moreover, the

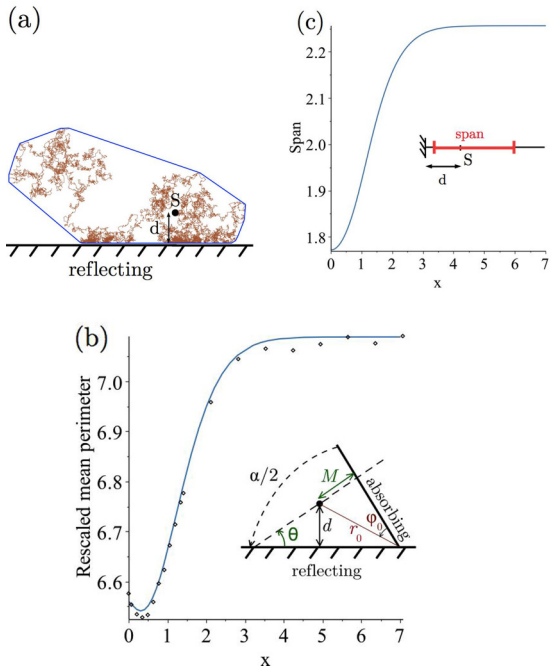

FIG. 1. (Color online) What is the influence of confinement on the convex hull of a 2D Brownian motion? Considering the minimal model of a reflecting confining infinite wall [see (a)], we show that the mean perimeter of the convex hull turns out to be a nonmonotonic function of the initial distance d to the wall [see (b)]. This is in striking contrast to the monotonic behavior of the mean span, which is the 1D analog of the mean perimeter of the convex hull [see (c)]. (a) Convex hull of a Brownian trajectory of starting point O and diffusion coefficient D. (b) Mean rescaled perimeter $\langle L^{(d)}_{2D}(t)/\sqrt{Dt}\rangle$ of the convex hull as a function of the rescaled distance to the wall $x = d/\sqrt{Dt}$: analytical (solid line) and simulation (dots) results (see Appendix C for details). The inset presents the different geometrical parameters involved in the calculation. (c) Mean rescaled span $\langle L^{(d)}_{1D}(t)/\sqrt{Dt}\rangle$ of a (semi)confined 1D Brownian motion as a function of the rescaled distance $x = d/\sqrt{Dt}$ to the reflecting point.

scaling function also exhibits an unexpected singularity as $x \to 0$, $\tilde{L}_{2D}(x) \sim -a\,[x/\ln(1/x)]^{3/2}$ with the prefactor $a = 8\sqrt{2\pi^3}/[3\Gamma(3/4)]$. We demonstrate that both the nonmonotonicity and the small x singularity of the scaling function are purely 2D effects and are, in fact, absent in one dimension [as shown in Fig. 1(c)].

One dimension. To get insight into the scaling function for the mean perimeter and to appreciate the fact that its nonmonotonicity and singularity at $x = 0$ are indeed induced by the 2D geometry, it is useful to first compute the analogous quantity in the one-dimensional (1D) setting, which is interesting in itself. In one dimension, the corresponding quantity is the mean span $\langle L^{(d)}_{1D}(t)\rangle$ of a Brownian motion on a semi-infinite line, starting at a distance d from a reflecting origin [see inset of Fig. 1(c)]. It can be expressed as

$$\left\langle L^{(d)}_{1D}(t)\right\rangle = \left\langle \mathcal{M}^{(d)}_{\rm right}(t)\right\rangle + \left\langle \mathcal{M}^{(d)}_{\rm left}(t)\right\rangle, \tag{2}$$

where $\langle \mathcal{M}^{(d)}_{\rm right}(t)\rangle$ and $\langle \mathcal{M}^{(d)}_{\rm left}(t)\rangle$ denote the mean maximal extensions of the walk up to time t to the right and to the left, respectively.

For convenience, we shift the reflecting wall to $-d$ and consider the walk starting at the origin S. We compute the right and the left parts separately, starting with the right. After integration by parts, it is found that $\langle \mathcal{M}^{(d)}_{\rm right}(t)\rangle = \int_0^\infty dy\ (1 - S^{(d)}_{\rm right}(t|y))$, where $S^{(d)}_{\rm right}(t|y) = {\rm Prob}[\mathcal{M}^{(d)}_{\rm right}(t) \leqslant y]$ is the cumulative distribution of $\mathcal{M}^{(d)}_{\rm right}(t)$, given that the particle starts at the origin. In turn, the cumulative distribution $S^{(d)}_{\rm right}(t|y)$ is just the probability that the walker starting at the origin stays within the box $[-d, y]$ up to time t, i.e., the survival probability of the walker with a reflecting wall at $-d$ and an absorbing wall at $y > 0$. In contrast, for the left side, the maximal displacement can, at most, be d due to the presence of the reflecting wall, and one finds $\langle \mathcal{M}^{(d)}_{\rm left}(t)\rangle = \int_{-d}^0 dy\ [1 - S_{\rm left}(t|y)]$, where $S_{\rm left}(t|y)$ is the survival probability of a walker in the semi-infinite region $[y, \infty[$ with an absorbing wall at $-d < y < 0$. These survival probabilities can be computed using standard techniques [21,23]. They are best expressed in terms of Laplace transforms with respect to t. Denoting by $\hat{f}(p) = \int_0^\infty f(t)\, e^{-p\,t}\, dt$ the Laplace transform of a function $f(t)$, we find

$$\begin{aligned} \left\langle \hat{\mathcal{M}}^{(d)}_{\rm right}(p)\right\rangle &= \int_0^{+\infty} dy \left(\frac{1}{p} - \hat{S}^{(d)}_{\rm right}(p|y)\right), \\ \left\langle \hat{\mathcal{M}}^{(d)}_{\rm left}(p)\right\rangle &= \int_{-d}^{0} dy \left(\frac{1}{p} - \hat{S}_{\rm left}(p|y)\right), \end{aligned} \tag{3}$$

where

$$\begin{aligned} \hat{S}^{(d)}_{\rm right}(p|y) &= \frac{1}{p}\left(1 - \frac{\cosh\left(\sqrt{\frac{p}{D}}d\right)}{\cosh\left[\sqrt{\frac{p}{D}}(y+d)\right]}\right), \\ \hat{S}_{\rm left}(p|y) &= \frac{1}{p}(1 - e^{\sqrt{\frac{p}{D}}y}). \end{aligned} \tag{4}$$

Inverting the Laplace transforms, we get

$$\begin{aligned} \tilde{\mathcal{M}}_{\rm right}(x) &\equiv \left\langle \frac{\mathcal{M}^{(d)}_{\rm right}(t)}{\sqrt{Dt}}\right\rangle \\ &= \frac{2}{\sqrt{\pi}} - 4\sum_{n=1}^{+\infty} \frac{(-1)^n}{4n^2-1}\left(\frac{e^{-n^2x^2}}{\sqrt{\pi}} - nx\,{\rm erfc}\,(nx)\right), \end{aligned} \tag{5}$$

$$\tilde{\mathcal{M}}_{\rm left}(x) \equiv \left\langle \frac{\mathcal{M}^{(d)}_{\rm left}(t)}{\sqrt{Dt}}\right\rangle = \frac{2}{\sqrt{\pi}}\left(1 - e^{-\frac{x^2}{4}}\right) + x\ {\rm erfc}\left(\frac{x}{2}\right), \tag{6}$$

with $x = d/\sqrt{Dt}$ denoting the scaled distance. This gives, from Eq. (2), $\langle L^{(d)}_{1D}(t)\rangle = \sqrt{D\,t}\ \tilde{L}_{1D}(\frac{d}{\sqrt{D\,t}})$, where the 1D scaling function, $\tilde{L}_{1D}(x) = \tilde{\mathcal{M}}_{\rm right}(x) + \tilde{\mathcal{M}}_{\rm left}(x)$, is plotted in Fig. 1(c). The scaling function increases monotonically with x from $\tilde{L}_{1D}(x \to 0) = \sqrt{\pi}$ (when the walker starts at the wall) to $\tilde{L}_{1D}(x \to \infty) = 4/\sqrt{\pi}$ (where the walker does not feel the wall and one recovers the mean span of the walker in the absence of the wall).

Several conclusions can be drawn from these expressions [see Fig. 1(c)]: (i) The presence of the reflecting wall preserves the diffusive scaling of the mean perimeter $\sim\sqrt{D\,t}$. (ii) However, for fixed d and late times, $\langle L_{1\mathrm{D}}^{(d)}(t)/\sqrt{Dt}\rangle \to \tilde{L}_{1\mathrm{D}}(x\to 0)=\sqrt{\pi}$, which is lower than $4/\sqrt{\pi}$ obtained in the absence of confinement ($d\to\infty$). (iii) The mean perimeter is minimized when the walker starts from the reflecting wall, and (iv) it is an increasing analytic function of the distance from the reflecting wall.

We show below that in two dimensions, while points (i) and (ii) continue to hold, (iii) and (iv) are no longer valid. Our main results are indeed the nonmonotonicity of the mean perimeter of the convex hull in two dimensions and its nonanalyticity for small starting distances from the reflecting wall. These two features are in striking contrast to the one-dimensional case derived above (see Fig. 1).

Two dimensions. We now turn to the 2D case, where we consider a Brownian motion in a semi-infinite medium (delimited by a reflecting wall) starting at a distance d from this wall [see Fig. 1(a)]. To compute the mean perimeter of the convex hull of the walk of duration t, we follow the general setup developed in Refs. [9,10]. By adapting Cauchy's formula [20] for the perimeter of closed convex curves to random curves, it was shown that the mean perimeter of the convex hull of any two-dimensional stochastic process, including that of a Brownian motion, can be expressed as [9,10]

$$\left\langle L_{2\mathrm{D}}^{(d)}(t)\right\rangle = \int_0^{2\pi} d\theta\ \langle \mathcal{M}^{(d)}(\theta,t)\rangle, \tag{7}$$

where $\mathcal{M}^{(d)}(\theta,t)$ is the maximal projection of the trajectory of the walker up to time t in the direction θ. As in the 1D case, it is useful to express the mean in terms of the cumulative distribution of $\mathcal{M}^{(d)}(\theta,t)$,

$$\langle \mathcal{M}^{(d)}(\theta,t)\rangle = \int_0^{+\infty} dM\ [1-S^{(d)}(t|M,\theta)], \tag{8}$$

where the cumulative distribution $S^{(d)}(t|M,\theta)$ can be identified to the survival probability up to time t of the walker in the semi-infinite plane, bounded additionally by an absorbing infinite wall at distance M from the starting point, perpendicular to the direction θ [see inset of Fig. 1(b)]. It then defines an infinite wedge of top angle $\alpha/2=\pi/2-\theta$ with one absorbing edge and one reflecting edge. However, by adding a twin wedge symmetrically around the reflecting edge, the survival probability of the walker in the original wedge is the same as in the "doubled" wedge with twice the top angle $\alpha=\pi-2\theta$, but with two absorbing edges. The survival probability of a Brownian walker, starting initially at the polar coordinates (r_0,φ_0), inside a wedge of angle α with two absorbing edges is [21]

$$S(t|r_0,\varphi_0) = \frac{r_0}{\sqrt{\pi\,Dt}}\, e^{-\frac{r_0^2}{8Dt}} \sum_{m=0}^{+\infty} \frac{\sin\left(\frac{(2m+1)\pi\varphi_0}{\alpha}\right)}{2m+1} \times\left[I_{\frac{(2m+1)\pi}{2\alpha}-\frac{1}{2}}\left(\frac{r_0^2}{8Dt}\right)+ I_{\frac{(2m+1)\pi}{2\alpha}+\frac{1}{2}}\left(\frac{r_0^2}{8Dt}\right)\right], \tag{9}$$

where $I_\nu(z)$ is the standard modified Bessel function. The initial position (r_0,φ_0) can be expressed in terms of the original variables M, d, and θ [see inset of Fig. 1(b)]. For convenience, we introduce two new dimensionless variables as $u\equiv M/\sqrt{Dt}=r_0\sin\varphi_0/\sqrt{Dt}$ and $x\equiv d/\sqrt{Dt}=r_0\sin(\alpha/2-\varphi_0)/\sqrt{Dt}$, where we recall that $\alpha=\pi-2\theta$. Then it follows that

$$\frac{r_0}{\sqrt{Dt}} = \frac{1}{\cos\theta}\sqrt{x^2+2xu\sin\theta+u^2}, \tag{10}$$

$$\varphi_0 = \arccos\left(\frac{x+u\sin\theta}{\sqrt{u^2+2xu\sin\theta+x^2}}\right). \tag{11}$$

Plugging the result for the survival probability in Eq. (9) [with r_0 and φ_0 expressed as functions of u and x via Eqs. (10) and (11)] into Eq. (8), we get

$$\begin{aligned}\tilde{\mathcal{M}}(\theta,x) &\equiv \left\langle\frac{\mathcal{M}^{(d)}(\theta,t)}{\sqrt{Dt}}\right\rangle \\ &= \int_0^{+\infty} du\left\{1-\frac{\sqrt{x^2+2xu\sin\theta+u^2}}{\sqrt{\pi}\cos\theta}\,\mathrm{e}^{-\frac{x^2+2xu\sin\theta+u^2}{8\cos^2\theta}}\right. \\ &\quad\times\sum_{m=0}^{\infty}\frac{\sin\left[(2m+1)\frac{\pi}{\alpha}\arccos\left(\frac{x+u\sin\theta}{\sqrt{u^2+2xu\sin\theta+x^2}}\right)\right]}{2m+1} \\ &\quad\times\left[I_\nu\left(\frac{x^2+2xu\sin\theta+u^2}{8\cos^2\theta}\right)\right. \\ &\quad\left.\left.+I_{\nu+1}\left(\frac{x^2+2xu\sin\theta+u^2}{8\cos^2\theta}\right)\right]\right\},\end{aligned} \tag{12}$$

with $\nu=(2m+1)\pi/(2\alpha)-1/2$. Integrating over θ in Eq. (7) then provides our final result for the mean rescaled perimeter (MRP):

$$\tilde{L}_{2\mathrm{D}}(x)\equiv\left\langle\frac{L_{2\mathrm{D}}^{(d)}(t)}{\sqrt{Dt}}\right\rangle=\int_0^{2\pi}d\theta\,\tilde{\mathcal{M}}(\theta,x), \tag{13}$$

with $\tilde{\mathcal{M}}(\theta,x)$ given explicitly in Eq. (12). As expected, the MRP is a function of only one parameter, the rescaled distance to the wall $x=d/\sqrt{Dt}$.

Interestingly, we show in Appendix A that the MRP, given in Eqs. (13) and (12) for arbitrary $x=d/\sqrt{Dt}$, simplifies a great deal in the important case of $x=0$ for a Brownian motion starting from the reflecting wall (or, equivalently, starting at any fixed distance but for large times):

$$\tilde{\mathcal{M}}(\theta,0)=2\sqrt{\pi}\,\frac{\cos\theta}{\pi-2\theta}. \tag{14}$$

As a simple check, we recover, for $\theta=0$ (i.e., in the direction parallel to the reflecting wall), the result for the nonconfined case $\tilde{\mathcal{M}}(0,0)=2/\sqrt{\pi}$. Indeed, the potential reflections on the wall do not affect the walk in the parallel direction. For $\theta=\pi/2$, outwards orthogonally to the wall, we recover the 1D result obtained above $\tilde{\mathcal{M}}(\pi/2,0)=\sqrt{\pi}$, which is higher than in the nonconfined case. Indeed, the wall pushes the trajectories farther in this direction. Finally, it is straightforward to obtain the MRP of the convex hull by integrating over the angle θ.

$$\tilde{L}_{2\mathrm{D}}(0)=2\sqrt{\pi}\,\mathrm{Si}(\pi)=6.56495\ldots, \tag{15}$$

where $\mathrm{Si}(z)=\int_0^z\frac{\sin x}{x}\,dx$. Note that the MRP for a walk starting from the reflecting wall still grows as $\sqrt{D\,t}$, but the prefactor $6.56495\ldots$ is lower than the nonconfined value $\sqrt{16\,\pi}=7.08982\ldots$.

As x increases from zero, the scaling function $\tilde{L}_{2\mathrm{D}}(x)$ in (13), supplemented by (12), first decreases, achieves a min-

imum, and then increases again before eventually saturating to the constant $\sqrt{16\,\pi}$ corresponding to the nonconfined case [see Fig. 1(b) for a plot]. This nonmonotonic behavior can already be understood by analyzing the $x \to 0^+$ limit. From Eq. (12), one can show that for small x (see Appendix B for details)

$$\tilde{\mathcal{M}}(\theta,x) - 2\sqrt{\pi}\,\frac{\cos\theta}{\pi - 2\theta} + \sin\theta x = \begin{cases} \frac{\sqrt{\pi}}{2}\frac{\cos\theta}{\pi-2\theta}x^2 + O(x^3) & \text{for} \quad \theta > 0, \\ C(\theta)\, x^{2\nu_0+2} + O(x^2) & \text{for} \quad \theta < 0, \end{cases} \tag{16}$$

where $\nu_0 = \theta/(\pi - 2\theta)$ and the amplitude $C(\theta)$ has a complicated expression (see Appendix B), which is negative for all $\theta < 0$. Interestingly, the leading order correction term in (16) is nonanalytic only for $\theta < 0$. Using Laplace's method, the integration over θ finally leads to

$$\tilde{L}(x) - 2\sqrt{\pi}\,\mathrm{Si}(\pi) \underset{x\ll 1}{\sim} -\frac{8\sqrt{2\pi^3}}{3\Gamma\left(\frac{3}{4}\right)}\left(\frac{x}{\ln(1/x)}\right)^{\frac{3}{2}}. \tag{17}$$

Let us make a few remarks: (i) While, for any fixed θ, $\tilde{\mathcal{M}}(\theta,x)$ has a nonzero linear term in x for small x, the linear term disappears when integrated over θ. (ii) Strikingly, the MRP is nonanalytic as $x \to 0$ (contrary to the 1D case), and (iii) it starts decreasing from a value at $x = 0$ which is lower than its $x \to \infty$ limit, so it must display a minimum, as confirmed in Fig. 1(b).

The existence of this surprising minimum can be qualitatively discussed by identifying the temporal regimes of a Brownian motion starting at a distance d from the reflecting wall: (i) At short times (i.e., $x \gg 1$), the walker does not see the reflecting wall, and the unconfined value of the MRP $4\sqrt{\pi}$ is recovered. (ii) After a time of order d^2/D (i.e., $x \simeq 1$), the reflecting wall starts impacting the trajectory by progressively reducing the space effectively accessible to the Brownian motion and thus decreasing the MRP. (iii) Next, these reflected trajectories start contributing to the outwards part of the convex hull (with respect to the plane). This effective repulsion is an antagonistic effect of the wall that turns out to increase the MRP. Finally, contrary to the 1D case, the MRP displays a complex behavior with x, involving a minimum. In addition, this minimum is global, implying in particular that the MRP is no longer minimized when the Brownian motion starts from the wall, but for a nontrivial value of $x \approx 0.3$.

Insights on this minimum may further be gained by considering the mean span in direction θ given by $\langle \mathcal{M}^{(d)}(\theta,t)\rangle + \langle \mathcal{M}^{(d)}(-\theta,t)\rangle$ involved in (7), whose small x development is obtained by combining the two forms of (16). Knowing that the mean span in direction θ at $x = 0$ is lower than its large x limit and that it starts decreasing [$C(\theta) < 0$], it displays a minimum for $\theta \neq 0$ and $\theta \neq \pi/2$ (see Fig. 2). After integration over θ, the nonmonotonicity remains.

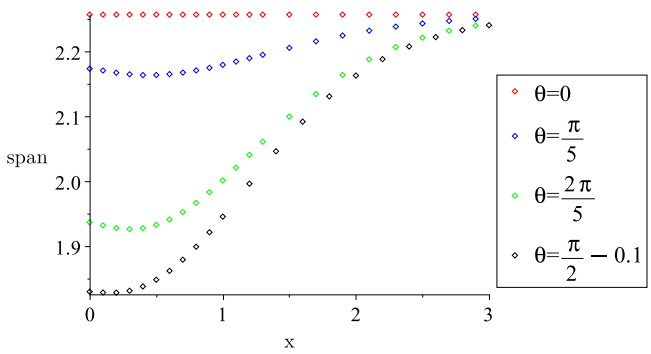

FIG. 2. (Color online) Mean span in direction θ as a function of the rescaled distance x for different values of θ. Like the mean perimeter of the convex hull, this quantity displays a minimum with respect to x for all directions except parallel or perpendicular to the wall.

In conclusion, we have studied analytically the mean perimeter of the convex hull of a Brownian motion in one and two dimensions in the presence of a reflecting wall at the origin. In two dimensions, this confinement leads to a striking nonmonotonic and nonanalytic (for small distances) behavior of the mean perimeter as a function of the scaled starting distance from the wall. The nonmonotonicity in 2D originates from the competition between two antagonistic effects due to the presence of the wall: reduction of the space accessible to the Brownian motion and effective repulsion. While these two effects are also at work in one dimension, they do not lead to a nonmonotonicity. Our work opens up several interesting questions for future studies. It would be interesting to know whether this nonmonotonicity persists in $d > 2$ dimensions. Computing the mean area of the convex hull in two dimensions in the presence of a reflecting wall remains challenging. Finally, it would be interesting to study other forms of confinements, for instance, a Brownian motion in an enclosed space or in the presence of an external confining potential.

Support from European Research Council Starting Grant No. FPTOpt-277998 is acknowledged. S.N.M. acknowledges support from ANR Grant No. 2011-BS04-013-01 WALKMAT.

APPENDIX A: DERIVATION OF $\tilde{\mathcal{M}}(\theta,0)$

We start from Eq. (12) in the main text and first rewrite the 1 on the right hand side (inside the integral) as

$$\frac{u}{\sqrt{\pi}\cos\theta}\, e^{-\frac{u^2}{8\cos^2\theta}} \sum_{m=0}^{+\infty} \frac{(-1)^m}{2m+1} 2 \frac{e^{\frac{u^2}{8\cos^2\theta}}}{\sqrt{2\pi\,\frac{u^2}{8\cos^2\theta}}} = 1. \tag{A1}$$

A change in variables and the introduction of a regularization parameter β yield

$$\tilde{\mathcal{M}}(\theta,0) = \frac{4}{\sqrt{\pi}}\cos\theta \sum_{m=0}^{\infty} \frac{(-1)^m}{2m+1} \underbrace{\int_0^{+\infty} dv\, e^{-\beta v}\left(\sqrt{\frac{2}{\pi}}\frac{e^v}{\sqrt{v}} - I_\nu(v) - I_{\nu+1}(v)\right)}_{A(\beta,m)}\Bigg|_{\beta=1}, \tag{A2}$$

where $A(\beta,m)$ can be shown to be given by

$$A(\beta,m) = \sqrt{\frac{2}{\beta-1}} - \frac{(\beta+\sqrt{\beta^2-1})^{-\nu}}{\sqrt{\beta^2-1}} - \frac{(\beta+\sqrt{\beta^2-1})^{-\nu-1}}{\sqrt{\beta^2-1}}. \tag{A3}$$

Using next that

$$\sum_{m=0}^{\infty} \frac{(-1)^m a^{-\frac{(2m+1)\pi}{2\alpha}+\frac{1}{2}}}{2m+1} = \sqrt{a}\arctan(a^{-\frac{\pi}{2\alpha}}) \tag{A4}$$

and taking the limit $\beta \to 1$ give the mean extension in the direction θ,

$$\tilde{\mathcal{M}}(\theta,0) = 2\sqrt{\pi}\frac{\cos\theta}{\pi-2\theta}. \tag{A5}$$

APPENDIX B: ASYMPTOTIC EXPANSION OF $\tilde{\mathcal{M}}(\theta,x)$ FOR SMALL DISTANCES

We give here the main steps for the derivation of the small x development of $\tilde{\mathcal{M}}(\theta,x)$ stated in Eq. (16) in the main text. The linear term in x (for $-\pi/2 < \theta < \pi/2$) and the quadratic term (for $0 < \theta < \pi/2$) are obtained by integration over u of the small x development of the survival probability. In turn, these integrals can be carried out by introducing, as performed in the calculation of the order 0 of $\tilde{\mathcal{M}}(\theta,x)$, a regularization factor β [see Eq. (A2)]. The integrals involved can be calculated straightforwardly. However, for $-\pi/2 < \theta < 0$, this method produces a diverging coefficient for the quadratic term, which reveals a nonanalytic behavior whose calculation is presented below.

The term T_0 responsible for the divergence is

$$T_0 = \int_0^{+\infty} du \left\{ \frac{2}{\pi} - \frac{\sqrt{u^2+2xu\sin\theta+x^2}}{\sqrt{\pi}\cos\theta} e^{-\frac{u^2+2xu\sin\theta+x^2}{8\cos^2\theta}} \times \cos\left[\frac{\pi}{\alpha}\arccos\left(\frac{u+x\sin\theta}{\sqrt{u^2+2xu\sin\theta+x^2}}\right)\right] \times I_{\nu_0}\left(\frac{u^2+2xu\sin\theta+x^2}{8\cos^2\theta}\right)\right\}, \tag{B1}$$

with $\nu_0 = \theta/(\pi-2\theta)$. The asymptotic behavior of T_0 can be conveniently analyzed by introducing the new variable of integration

$$z = \frac{u^2+2xu\sin\theta+x^2}{x^2\cos^2\theta}. \tag{B2}$$

It leads to

$$\begin{aligned} T_0 &= \int_1^{1/\cos^2\theta} dz \frac{x\cos\theta}{2\sqrt{z-1}} \left\{ \frac{2}{\pi} - \frac{x}{\sqrt{\pi}}\sqrt{z}\cos\left[\frac{\pi}{\alpha}\arccos\left(-\frac{\sqrt{z-1}}{\sqrt{z}}\right)\right] e^{-\frac{x^2 z}{8}} \mathrm{I}_{\nu_0}\left(\frac{x^2 z}{8}\right)\right\} \\ &\quad + \int_1^{+\infty} dz \frac{x\cos\theta}{2\sqrt{z-1}} \left\{ \frac{2}{\pi} - \frac{x}{\sqrt{\pi}}\sqrt{z}\cos\left[\frac{\pi}{\alpha}\arccos\left(\frac{\sqrt{z-1}}{\sqrt{z}}\right)\right] e^{-\frac{x^2 z}{8}} \mathrm{I}_{\nu_0}\left(\frac{x^2 z}{8}\right)\right\} \\ &\equiv I_1 + I_2. \end{aligned} \tag{B3}$$

The first integral I_1 can be written as

$$I_1 = -\frac{2x}{\pi}\sin\theta - \frac{x^2\cos\theta}{2\sqrt{\pi}} \int_1^{1/\cos^2\theta} dz \sqrt{\frac{z}{z-1}} \cos\left[\frac{\pi}{\alpha}\arccos\left(-\frac{\sqrt{z-1}}{\sqrt{z}}\right)\right] e^{-\frac{x^2 z}{8}} I_{\nu_0}\left(\frac{x^2 z}{8}\right). \tag{B4}$$

The second integral I_2 cannot be split as it leads to two diverging contributions. Subtracting to the integrand the order 0 given by

$$\int_0^{+\infty} dz \frac{x\cos\theta}{2\sqrt{z}} \left[\frac{2}{\pi} - \frac{x}{\sqrt{\pi}}\sqrt{z}\, e^{-\frac{x^2 z}{8}} \mathrm{I}_{\nu_0}\left(\frac{x^2 z}{8}\right)\right] = 4\,\nu_0 \frac{\cos\theta}{\sqrt{\pi}}, \tag{B5}$$

we obtain

$$\begin{aligned} I_2 &= 4\,\nu_0\frac{\cos\theta}{\sqrt{\pi}} + \int_1^{+\infty} dz \frac{x\cos\theta}{\pi}\left(\frac{1}{\sqrt{z-1}} - \frac{1}{\sqrt{z}}\right) - \frac{x^2\cos\theta}{2\sqrt{\pi}} \int_1^{+\infty} dz \left\{\sqrt{\frac{z}{z-1}}\cos\left[\frac{\pi}{\alpha}\arccos\left(\sqrt{\frac{z-1}{z}}\right)\right] - 1\right\} \\ &\quad \times e^{-\frac{x^2 z}{8}} \mathrm{I}_{\nu_0}\left(\frac{x^2 z}{8}\right) - \int_0^1 dz \frac{x\cos\theta}{2\sqrt{z}}\left[\frac{2}{\pi} - \frac{x}{\sqrt{\pi}}\sqrt{z}\, e^{-\frac{x^2 z}{8}} \mathrm{I}_{\nu_0}\left(\frac{x^2 z}{8}\right)\right]. \end{aligned} \tag{B6}$$

This finally yields

$$T_0 = \frac{4\theta\cos\theta}{\sqrt{\pi}(\pi-2\theta)} - \frac{2x}{\pi}\sin\theta + \mathrm{C}(x,\theta), \tag{B7}$$

with

$$C(x,\theta) = \frac{x^2\cos\theta}{2\sqrt{\pi}}\left\{\int_0^1 dz\ e^{-\frac{x^2 z}{8}}\ I_{\nu_0}\left(\frac{x^2 z}{8}\right) - \int_1^{1/\cos^2\theta} dz\,\sqrt{\frac{z}{z-1}}\cos\left[\frac{\pi}{\alpha}\arccos\left(-\frac{\sqrt{z-1}}{\sqrt{z}}\right)\right]\times\ e^{-\frac{x^2 z}{8}}\ I_{\nu_0}\left(\frac{x^2 z}{8}\right)\right.$$
$$\left. - \int_1^{+\infty} dz\,\left\{\sqrt{\frac{z}{z-1}}\cos\left[\frac{\pi}{\alpha}\arccos\left(\sqrt{\frac{z-1}{z}}\right)\right] - 1\right\} e^{-\frac{x^2 z}{8}}\ I_{\nu_0}\left(\frac{x^2 z}{8}\right)\right\}. \tag{B8}$$

The constant and linear terms of Eq. (B7) contribute to give the constant and linear terms of Eq. (16) of the main text. As for the last term, we use the development of the integrand of Eq. (B8) for small x,

$$e^{-\frac{x^2 z}{8}}\ I_{\nu_0}\left(\frac{x^2 z}{8}\right) \underset{x\to 0}{\sim} \frac{x^{2\nu_0} z^{\nu_0}}{16^{\nu_0}\Gamma(1+\nu_0)} + O(x^{2+2\nu_0}) \tag{B9}$$

to obtain

$$C(x,\theta) \underset{x\to 0}{\sim} C(\theta) x^{2+2\nu_0} + O(x^2), \tag{B10}$$

where

$$C(\theta) = \frac{\cos\theta}{2\sqrt{\pi}16^{\nu_0}\Gamma(1+\nu_0)}\left(\frac{1}{1+\nu_0} - \int_1^{1/\cos^2\theta} dz\,\sqrt{\frac{z}{z-1}}\cos\left[\frac{\pi}{\alpha}\arccos\left(-\frac{\sqrt{z-1}}{\sqrt{z}}\right)\right] z^{\nu_0}\right.$$
$$\left. - \int_1^{+\infty} dz\,\left\{\sqrt{\frac{z}{z-1}}\cos\left[\frac{\pi}{\alpha}\arccos\left(\sqrt{\frac{z-1}{z}}\right)\right] - 1\right\} z^{\nu_0}\right). \tag{B11}$$

Replacing ν_0 and α with their values θ/α and $\pi - 2\theta$ finally leads to the small x development of $\tilde{M}(\theta,x)$ for $-\pi/2 < \theta < 0$ [see Eq. (16) of the main text].

$$\tilde{M}(x) = \frac{2\sqrt{\pi}\cos\theta}{\pi - 2\theta} - \sin\theta\, x + C(\theta) x^{2+\frac{2\theta}{\pi-2\theta}} + O(x^2). \tag{B12}$$

APPENDIX C: NUMERICAL SIMULATIONS

We computed the mean perimeter of the convex hull of a Brownian motion via numerical simulations. We constructed Gaussian random walks of 10^5 steps with a time step $\Delta\tau = 10^{-3}$ when the walker is farther than a distance $d \simeq 0.2$ from the wall. When the walker approaches the wall, we take an adapted time step quadratic in the distance d to the wall $\Delta\tau = (0.1\,d + \lambda)^2$ with $\lambda = 0.01$. The parameter λ should not be too small to prevent the computation time from diverging. The convex hull is then constructed using the Graham scan algorithm (see Ref. [24]) for each Brownian walk, with its perimeter calculated and averaged over 10^5 realizations. Agreement is found with our analytical prediction [see Fig. 1(b)].

[1] H. C. Berg, *Random Walks in Biology* (Princeton University Press, Princeton, NJ, 1983); L. Edelstein-Keshet, *Mathematical Models in Biology* (McGraw-Hill, Boston, 1988).
[2] F. Bartumeus, M. G E. da Luz, G. M. Viswanathan, and J. Catalan, Ecology **86**, 3078 (2005).
[3] D. Murphy and B. Noon, Ecol. Appl. **2**, 3 (1992).
[4] B. J. Worton, Biometrics **51**, 1206 (1995).
[5] L. Giuggioli, J. R. Potts, and S. Harris, PLoS Comput. Biol. **7**, e1002008 (2011).
[6] L. Takács, Am. Math. Mon. **87**, 142 (1980).
[7] M. El Bachir, Ph.D. thesis, Université Paul Sabatier, 1983.
[8] G. Letac, J. Theor. Probab. **6**, 385 (1993).
[9] J. Randon-Furling, S. N. Majumdar, and A. Comtet, Phys. Rev. Lett. **103**, 140602 (2009).
[10] S. N. Majumdar, A. Comtet, and J. Randon-Furling, J. Stat. Phys. **138**, 955 (2010).
[11] A. Reymbaut, S. N. Majumdar, and A. Rosso, J. Phys. A **44**, 415001 (2011).
[12] E. Dumonteil, S. N. Majumdar, A. Rosso, and A. Zoia, Proc. Natl. Acad. Sci. USA **110**, 4239 (2013).
[13] J. Randon-Furling, J. Phys. A **46**, 015004 (2013).
[14] M. Luković, T. Geisel, and S. Eule, New J. Phys. **15**, 063034 (2013).
[15] J. Randon-Furling, Phys. Rev. E **89**, 052112 (2014).
[16] P. Biane and G. Letac, J. Theor. Probab. **24**, 330 (2011).
[17] R. Eldan, Elec. J. Probab. **19**, 1 (2014).
[18] J. Kampf, G. Last, and I. Molchanov, Proc. Am. Math. Soc. **140**, 2527 (2012).
[19] Z. Kabluchko and D. Zaporozhets, arXiv:1404.6113.
[20] A. Cauchy, *La rectification des courbes*, Mémoire de l'Académie des Sciences (Académie des Sciences, Paris, 1832).
[21] S. Redner, *A Guide to First-Passage Processes* (Cambridge University Press, Cambridge, 2001).
[22] G. Barton, *Elements of Green's Functions and Propagation* (Clarendon, Oxford, 1989).
[23] A. J. Bray, S. N. Majumdar, and G. Schehr, Adv. Phys. **62**, 3 (2013).
[24] R. L. Graham, Inf. Process. Lett. **1**, 132 (1972).